Computational Sciences and Engineering 2(1) (2022) 81-95

University of Guilan

Computational Sciences and Engineering

journal homepage: https://cse.guilan.ac.ir/

Analytical Investigations of Vehicle Dynamic Behaviours under Influence of Magnetorheological Fluid Damper

A. I. Adeleke [a], M. A. Waheed [a], S. I. Kuye [a], B. I. Olajuwon [a], M.G. Sobamowo [b,*]

[a] Department of Mechanical Engineering, Federal University of Agriculture, Abeokuta, Ogun State, Nigeria.

[b] Department of Mechanical Engineering, University of Lagos, Akoka, Lagos, Nigeria.

ARTICLE INFO

Article history:
Received 20 March 2022
Received in revised form 28 April 2022
Accepted 29 April 2022
Available online 31 April 2022

Keywords:
Magnetorheological fluid damper
Vehicle dynamics
Vehicle suspension system
Analytical Investigations

ABSTRACT

The present study focusses on the developments of analytical solutions for vehicle dynamic behaviour under the influence of magnetorheological fluid damper. Dynamic models of a quarter vehicle are considered. Also, the damping force of the magnetorheological fluid damper are modelled using Bouc-Wen and modified Bouc-Wen models. The developed vibration models for the study of the dynamic behaviour of the vehicle are solved using Laplace transform method. The parametric studies reveal that the oscillation of the displacement of the axle is more fluctuating compared to the displacement of the body due to the installation of the damper between the body and the axle in which the damper acts as a shock-absorber. Moreover, the variation between the two models of Bouc-Wen and modified Bouc-Wen models are established. It is analytically validated that the Bouc-Wen model cannot produce the experimentally observed roll-off in the yield region for velocities with a small absolute value and operational sign opposite to the sign of the acceleration. Therefore, the use of modified Bouc-Wen model is recommended. It is hoped that the developed exact analytical models will serve as basis for comparisons of any other method of analysis of the problem.

1. Introduction

The stability, comfortable capability and safety of a vehicle are directly related to the suspension system [1]. Typically, the suspension system of a vehicle is made up of springs and shock absorbers which help to isolate the vehicle chassis and occupants from sudden vertical displacements of the wheel assemblies during driving. A well-tuned suspension system is important for the comfort and safety of the vehicle occupants as well as the long-term durability of the vehicle's electronic and

* Corresponding author.
E-mail address: mikegbeminiyiprof@yahoo.com (M.G. Sobamowo)

http://dx.doi.org/10.22124/cse.2022.21991.1029

mechanical components. The suspension system of a vehicle can be (i) ppassive ssuspension ssystem (ii) semi-active ssuspension system (iii) active ssuspension system. The different types are shown in Figure 1.

The passive suspension system shown in Figure 1a does not have capability of controlling suspension stiffness and damping coefficient according to the road roughness or the disturbance amplitude. Also, in passive suspension system, the characteristics of the spring and the damper (which are determined according to the performance goals and its intended applications) are fixed [3]. Figure 1b depicts semi-active suspension system which has advantages over the passive suspension in terms of spring stiffness and damping coefficient control according to road roughness and disturbances experienced by the unsprung mass of the vehicle. Since such system does not possess the separate dynamic control component for the operation of suspension against the road disturbances, it processes the road roughness/disturbances based on the suspension travel sensor feedback. In such system, the state of the particular suspension is baselined on the signals received from the road disturbances. Semi-active suspension system has a controllable damper that facilitates the improved handling of the vehicle, better comfort to driver and passenger as compared to the passive suspension system [3]. The recent derivation of the suspension technology is made of active suspension system which has a dedicated dynamic control component for operation of suspension against the road roughness/ disturbance. Such system requires constant power source, transmission mechanism for the generated force by power source, and sensory network and microcontroller for the control mode selection. The suspension system possesses the capability to vary damping force required for the ride comfort against the road disturbances experienced by the vehicle. Multiple control mode operation to compensate for the variety of the road roughness facilitates improved vehicle handling performance, and thus achieves the better stability of the vehicle compared to passive and semi-active suspension systems. Also, cornering abilities are enhanced due to the reactive inertia applied against the spring deformation while turning. The typical configuration of the suspension is shown in Figure 1c [3].

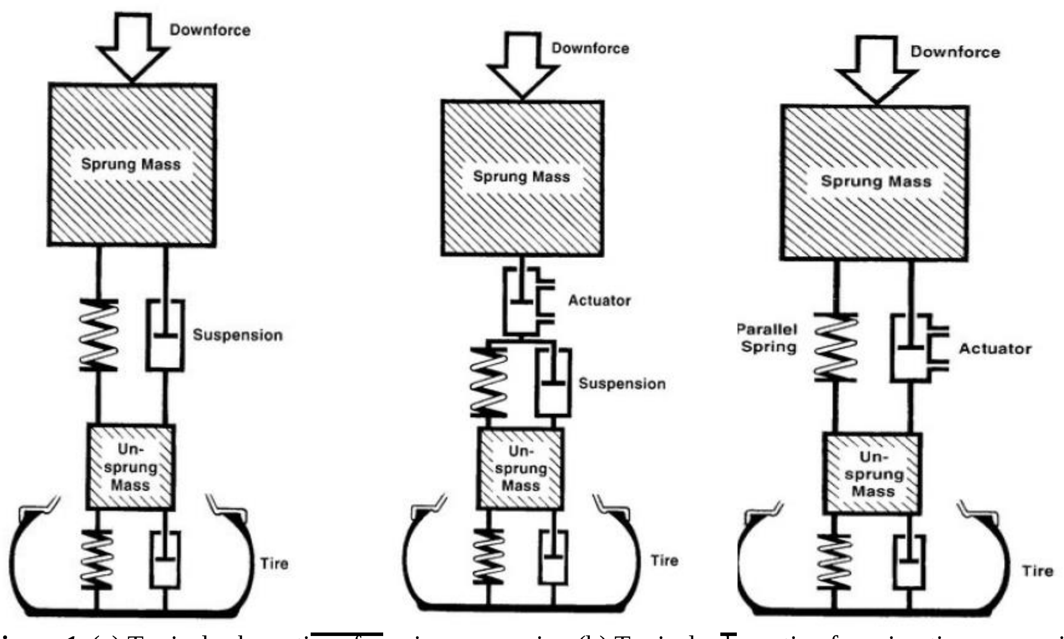

Figure 1. (a) Typical schematics of passive suspension (b) Typical schematic of semi-active suspension schematics (c)Typical schematic of active suspension schematics [2]

Magnetorheological fluid damper includes magnetorheological fluid, a pair of wires, a housing, a piston, a magnetic coil, and an accumulator as shown in Figure 2.

Magnetorheological (MR) fluids are fluids that consist of small particles of iron (in the order of μm) magnetizable, suspended in oil, generally hydrocarbon. Also, some additives are added to the fluid with objective to inhibit the deposit of iron particles, to promote its suspension, to modify viscosity and to diminish the consuming. One excellent characteristics of magnetorheological fluid is that its rheological characteristics changes when magnetic field is applied. The intensity of applied magnetic field is used to control the viscosity of the fluid. The special behavior of magnetorheological fluid has resulted in its vast of applications such as dampers, shock absorbers, rotary brakes, prosthetic devices, clutches, polishing and grinding devices, etc. Among these applications, magnetorheological fluid dampers, which utilize the advantages of magnetorheological fluids, are semi-active control devices that are widely used in the modern industry nowadays.

In magnetorheological fluid damper, the MR fluid is housed within the cylinder and flows through a small orifice. The magnetic coil is built in the piston or on the housing. When a current is supplied to the coil, the particles are aligned and the fluid changes from the liquid state to the semi-solid state within milliseconds. Consequently, a controllable damping force is produced.

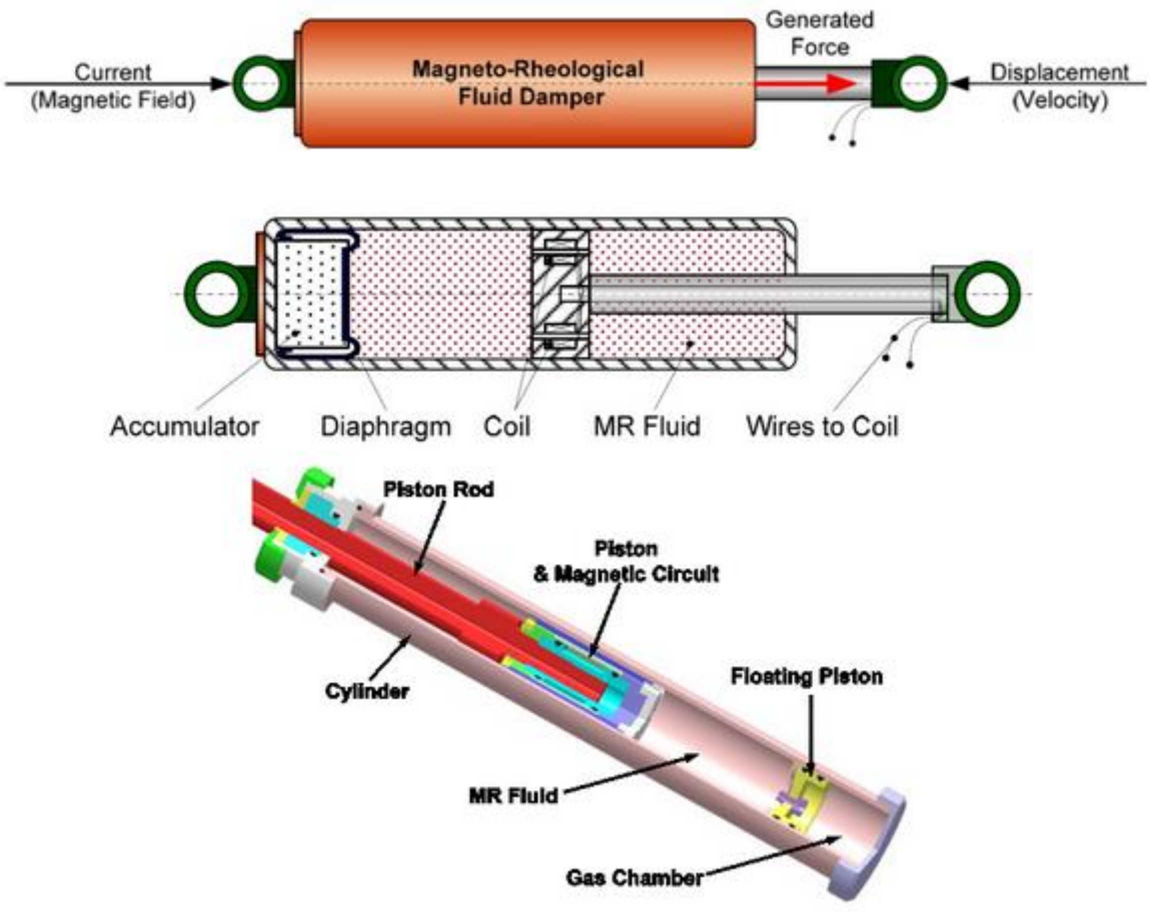

Figure 2. General configuration of a MR fluid damper [4]

Parametrically, Wereley et al. [5] opined that magnetohydrodynamic dampers can be classified as Bingham-based dynamic models, the Bi-viscous models, the Viscoelastic-Plastic models, the Stiffness-Viscosity-Elasto-Slide models. Ikhouane and Dyke [6] modelled the shear mode of magnetorheological damper using the Bouc-wen dynamic models. Jimnez and Alvarez [7], Sakai et al. [8] and Terasawa et al. [9] adopted LuGre hysteresis operator-based models to analyze the dynamic behaviours of magnetorheological dampers for vibration control. Kwok et al. [10] utilized hyperbolic tangent function-based models while Wang et al. [11] and Ma et al. [12] applied Sigmoid function-based models for hysteretic behaviour of a magnetorheological fluid damper. Oh [13] experimented the hysteretic characteristics of a magnetorheological fluid damper using the equivalent models. Wang and Kamath [14] modelled the hysteretic characteristics of a magnetorheological fluid damper using Phase Transition models. Spencer et al. [15] presented the phenomenological models for dynamic behaviours of magnetorheological dampers while Yang et al. [16] modelled and analyzed dynamic performance of large-scale magnetorheological fluid dampers. Wereley et al. [17] modelled the vibration of electrorheological and magnetorheological fluid dampers while Pang et al. [18] studied a linear stroke magnetorheological fluid damper. Snyder et al. [19] explored the magnetorheological fluid damper behaviour under the influence of sinusoidal loading. Other studies on the vibrational behaviour od structures under the influences of magnetorheological fluid damper are given in [20-29].

The dynamic models of the above reviewed studies have been analyzed using numerical methods. However, the classical way of finding analytical solutions to linear and nonlinear models are obviously still very important. This is because such symbolic solutions serve as accurate benchmarks for numerical solutions. Exact analytical solutions are essential for the developments of efficient tools of applied numerical simulations. Inevitably, analytical expressions show the direct relationship between the models' parameters. They provide good insights into the importance of various parameters of the system that affect the phenomena. It enhances reduction in the computation and simulation costs of real-life problems. Therefore, in this work, exact analytical solutions are developed for the vehicle dynamic behaviour under the influence of magnetorheological damper. Dynamic models for a quarter vehicle are considered and the damping force of the MR damper are modelled using Bouc-Wen and modified Bouc-Wen models. The developed vibration models for the study of the dynamic behaviour of the vehicle are solved using Laplace transform method. Comparison of the results of the two models are analyzed and discussed.

2. Model Development: A Quarter Car Model of vehicle suspension system

Consider a quarter car model as a two degree-of-freedom suspension system as shown in Figure 3. In the figure, the vehicle mass with passenger is represented by a sprung mass m_1 and the mass of wheels and associated components are represented by an unsprung mass m_2. The vertical motion of the system can be described by the displacement x_1 and x_2. The excitation due to road disturbance is x_b. The suspension spring constant is ks_1 and the tire spring constant is ks_2. Moreover, the damping force for the MR damper and damping coefficient of the tire are f_d and dr_2, respectively.

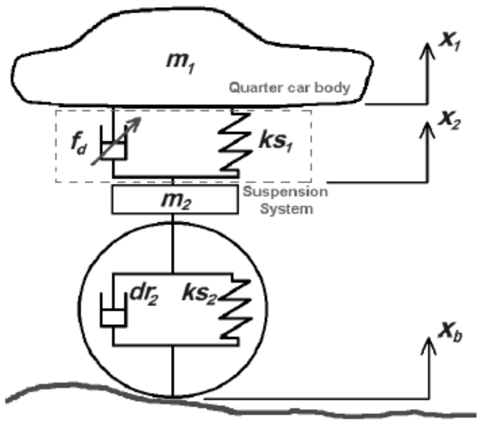

Figure 3. Mechanical model of a quarter car model vehicle suspension system [31]

$$m_1 \frac{d^2 x_1}{dt^2} + ks_1 (x_1 - x_2) + f_d = 0 \tag{1}$$

$$m_2 \frac{d^2 x_2}{dt^2} - dr_2 \left(\frac{dx_b}{dt} - \frac{dx_2}{dt} \right) - ks_1 (x_1 - x_2) - ks_2 (x_b - x_2) - f_d = 0 \tag{2}$$

The initial conditions are

$$x_1 = x_{1,0},\ \ x_2 = x_{2,0},\ \ \frac{dx_1}{dt} = 0,\ \frac{dx_2}{dt} = 0,\ \ when\ \ t = 0 \tag{3}$$

where m_1 *and* m_2 are the masses of the vehicle body and suspension, respectively, ks_1 is the total stiffness coefficient of the suspension, including the effective stiffness of the MR damper, dr_1 is the damping coefficient of the suspension, ks_2 is the vertical stiffness of the tyre, dr_2 is the damping coefficient of the tyre and x_1 , x_2 and x_b are the vertical displacements of sprung mass (the vehicle body), unsprung mass (the tyre) and road excitation, respectively and f_d is the damping force [31].

2.1 Modeling Road Profile for the Wheel Vertical Dynamics Behaviour

The road is not a smooth terrain, and the profile has to be considered in the dynamic model [30]. The simplest form of the road profile is sinusoidal shape as shown in Figure 4.

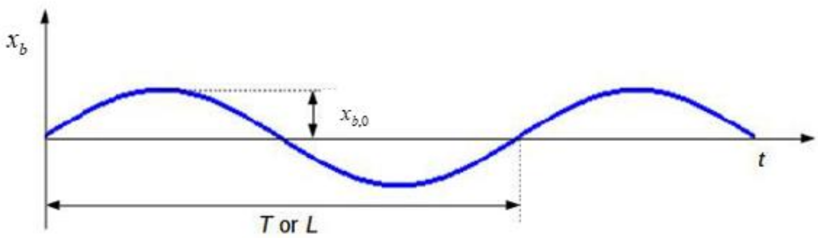

Figure 4. Sinusoidal profile of road irregularities

The model for the profile is given as

$$x_b = x_{b,0} sin(\omega t + \varepsilon) \quad (4)$$

Where the angular frequency (rad/)s is given by

$$\omega = \frac{2\pi v}{L} \quad (5)$$

ε is the phase offset

L is road irregularity length

Many times, the road profile is not perfect sinusoidal shape. A periodic signal as a sum of several harmonics can be used to develop a more realistic road profile as shown in Figure 5. The mathematical model is given as Fourier series which is a sum of sine functions with different frequencies and amplitudes

$$x_b = h_0 + \sum_{n=1}^{N} h_n sin(n\omega t + \varepsilon_n) \quad (6)$$

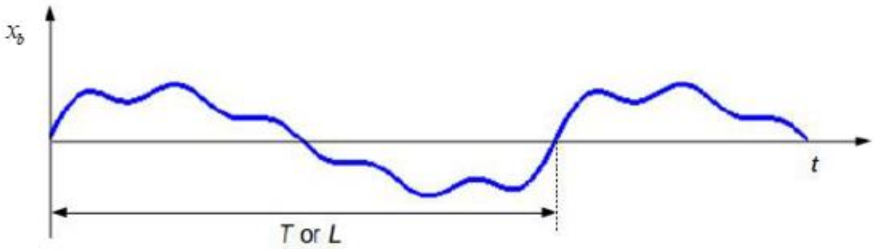

Figure 5. Periodical profile of road irregularities

Furthermore, in realities, most road profiles cannot be expressed as periodic functions. The height of the road in time is random (stochastic). Figure 6 presents such road profile.

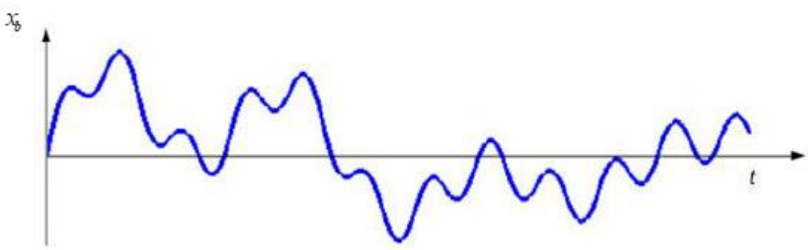

Figure 6 Stochastic profile of road irregularities

2.2 Modeling the Damping Force for the Magnetorheological fluid damper

The behaviour of the magnetorheological fluid damper can be modelled using the Bouc-Wen model. The Bouc-Wen model is given as in Figure 7.

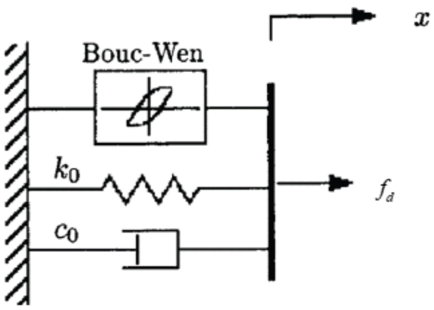

Figure 7. Bouc-Wen Model [15, 20]

The mathematical description of the system with the magnetorheological fluid damper is given as

$$f_d = c_0\dot{x} + k_0(x - x_0) + \alpha z \quad (7)$$

where the hysteresis component z satisfies the

$$\dot{z} = -\gamma|\dot{x}||z|^{n-1} z - \beta\dot{x}|z|^n + \delta\dot{x} \quad (8)$$

However, the classical Bouc-Wen model cannot produce the experimentally observed roll-off in the yield region for velocities with a small absolute value and operational sign opposite to the sign of the acceleration [29,34]. Therefore, in this work, the behaviour of the magnetorheological fluid damper can be characterized using the modified Bouc-Wen model shown in Figure 8.

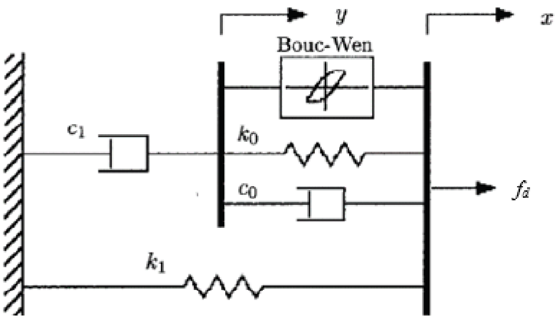

Figure 8. Modified Bouc-Wen Model [15, 20]

The model for the magnetorheological damping force is given as

$$f_d = \alpha z + c_0(\dot{x} - \dot{y}) + k_0(x - y) + k_1(x - x_0) \quad (9)$$

where

$$\dot{y} = \frac{1}{(c_0 + c_1)}\left[\alpha z + k_0(x - y) + c_0\dot{x}\right] \quad (10)$$

and

$$\dot{y} = -\gamma\left|\dot{x}-\dot{y}\right|\left|z\right|^{n-1} z - \beta\left(\dot{x}-\dot{y}\right)\left|z\right|^{n} + \delta\left(\dot{x}-\dot{y}\right) \tag{11}$$

It can be found from Eq. (10) that

$$c_1\dot{y} = \alpha z + c_0(\dot{x}-\dot{y}) + k_0(x-y) \tag{12}$$

Therefore, Eq. (9) can be written as

$$f_d = c_1\dot{y} + k_1(x-x_0) \tag{13}$$

where

$$c_1 = c_{1a} + c_{1b}u \tag{14}$$

and

$$\dot{u} = -\eta\left(u-V\right) \tag{16}$$

3. Analytical Solutions to the Developed Dynamic Equations

Analytical solutions can be developed for Equs. (1) and (2) using Laplace transform method. The application of the Laplace transform to the equations are shown as follows:

$$m_1\left(s^2\overline{x}_1 - sx_{1,0}\right) + ks_1\left(\overline{x}_1 - \overline{x}_2\right) + \overline{f}_d = 0 \tag{17}$$

$$m_2\left(s^2\overline{x}_2 - sx_0\right) - dr_2\left(\left(s\overline{x}_b - x_{b,0}\right) - \left(s\overline{x}_2 - x_{2,0}\right)\right) - ks_1\left(\overline{x}_1 - \overline{x}_2\right) - ks_2\left(\overline{x}_b - \overline{x}_2\right) - \overline{f}_d = 0 \tag{18}$$

where

$$\overline{f}_d = c_1 s\left(\overline{y} - y_0\right) + k_1\left(\overline{x} - \frac{x_0}{s}\right) \tag{19}$$

Then we have

$$\left(m_1 s^2 + ks_1\right)\overline{x}_1 - ks_1\overline{x}_2 = m_1 s x_{1,0} - \overline{f}_d \tag{20}$$

$$-ks_1\bar{x}_1+\left(m_2s^2-dr_2s+ks_1+ks_2\right)\bar{x}_2=\bar{f}_d+m_2sx_0-dr_2x_{2,0}-dr_2x_{b,0}+\left(dr_2s+ks_2\right)\bar{x}_b \tag{21}$$

Which can be written in Matrix form as

$$\begin{bmatrix}\left(m_1s^2+ks_1\right) & -ks_1\\ -ks_1 & \left(m_2s^2-dr_2s+ks_1+ks_2\right)\end{bmatrix}\begin{bmatrix}\bar{x}_1\\ \bar{x}_2\end{bmatrix}=\begin{bmatrix}m_1sx_{1,0}-\bar{f}_d\\ \bar{f}_d+m_2sx_0-dr_2x_{2,0}-dr_2x_{b,0}+\left(dr_2s+ks_2\right)\bar{x}_b\end{bmatrix} \tag{22}$$

On solving the above equations using Crammer's rule, we have

$$\bar{x}_1=\frac{\left(m_2s^2-dr_2s+ks_1+ks_2\right)\left(m_1sx_{1,0}-\bar{f}_d\right)+\left(\bar{f}_d+m_2sx_0-dr_2x_{2,0}-dr_2x_{b,0}+\left(dr_2s+ks_2\right)\bar{x}_b\right)\left(ks_1\right)}{\left(m_2s^2-dr_2s+ks_1+ks_2\right)\left(m_1s^2+ks_1\right)-\left(ks_1\right)^2} \tag{23}$$

$$\bar{x}_2=\frac{\left(m_1s^2+ks_1\right)\left(\bar{f}_d+m_2sx_0-dr_2x_{2,0}-dr_2x_{b,0}+\left(dr_2s+ks_2\right)\bar{x}_b\right)+\left(m_1sx_{1,0}-\bar{f}_d\right)\left(ks_1\right)}{\left(m_2s^2-dr_2s+ks_1+ks_2\right)\left(m_1s^2+ks_1\right)-\left(ks_1\right)^2} \tag{24}$$

Due to the complexity in finding the inverse Laplace transforms of Eqs. (23) and (24), a numerical evaluation of the inverse Laplace transform is carried out using Simon's approach [32] given as

$$x_1(t)=\frac{e^{a_pt}}{t}\left[\frac{1}{2}\bar{x}_1\left(a_p\right)+\sum_{n=1}^{N}Re\left[\bar{x}_1\left(a_p+i\frac{n\pi}{a_p}\right)\right]\left(-1\right)^n\right] \tag{25}$$

$$x_2(t)=\frac{e^{a_pt}}{t}\left[\frac{1}{2}\bar{x}_2\left(a_p\right)+\sum_{n=1}^{N}Re\left[\bar{x}_2\left(a_p+i\frac{n\pi}{a_p}\right)\right]\left(-1\right)^n\right] \tag{26}$$

where

$$\bar{x}_1(a_p)=\frac{\left(m_2a_p{}^2-dr_2a_p+ks_1+ks_2\right)\left(m_1x_{1,0}a_p-\bar{f}_d\right)+\left(\bar{f}_d+m_2x_0a_p-dr_2x_{2,0}-dr_2x_{b,0}+\left(dr_2a_p+ks_2\right)\bar{x}_b\right)\left(ks_1\right)}{\left(m_2a_p{}^2-dr_2a_p+ks_1+ks_2\right)\left(m_1a_p{}^2+ks_1\right)-\left(ks_1\right)^2}$$

$$\bar{x}_2(a_p)=\frac{\left(m_1a_p{}^2+ks_1\right)\left(\bar{f}_d+m_2x_0a_p-dr_2x_{2,0}-dr_2x_{b,0}+\left(dr_2a_p+ks_2\right)\bar{x}_b\right)+\left(m_1x_{1,0}a_p-\bar{f}_d\right)\left(ks_1\right)}{\left(m_2a_p{}^2-dr_2a_p+ks_1+ks_2\right)\left(m_1a_p{}^2+ks_1\right)-\left(ks_1\right)^2}$$

$$\bar{x}_1\left(a_p+i\frac{n\pi}{a_p}\right)=\frac{\left[\begin{array}{l}\left(m_2\left(a_p+i\frac{n\pi}{a_p}\right)^2-dr_2\left(a_p+i\frac{n\pi}{a_p}\right)+ks_1+ks_2\right)\left(m_1x_{1,0}\left(a_p+i\frac{n\pi}{a_p}\right)-\bar{f}_d\right)\\+\left(\bar{f}_d+m_2x_0\left(a_p+i\frac{n\pi}{a_p}\right)-dr_2x_{2,0}-dr_2x_{\mathrm{b},0}+\left(dr_2\left(a_p+i\frac{n\pi}{a_p}\right)+ks_2\right)\bar{x}_b\right)(ks_1)\end{array}\right]}{\left(m_2\left(a_p+i\frac{n\pi}{a_p}\right)^2-dr_2\left(a_p+i\frac{n\pi}{a_p}\right)+ks_1+ks_2\right)\left(m_1\left(a_p+i\frac{n\pi}{a_p}\right)^2+ks_1\right)-(ks_1)^2}$$

$$\bar{x}_2\left(a_p+i\frac{n\pi}{a_p}\right)=\frac{\left[\begin{array}{l}\left(m_1\left(a_p+i\frac{n\pi}{a_p}\right)^2+ks_1\right)\left(\begin{array}{l}\bar{f}_d+m_2x_0\left(a_p+i\frac{n\pi}{a_p}\right)-dr_2x_{2,0}\\-dr_2x_{\mathrm{b},0}+\left(dr_2\left(a_p+i\frac{n\pi}{a_p}\right)+ks_2\right)\bar{x}_b\end{array}\right)\\+\left(m_1x_{1,0}\left(a_p+i\frac{n\pi}{a_p}\right)-\bar{f}_d\right)(ks_1)\end{array}\right]}{\left(m_2\left(a_p+i\frac{n\pi}{a_p}\right)^2-dr_2\left(a_p+i\frac{n\pi}{a_p}\right)+ks_1+ks_2\right)\left(m_1\left(a_p+i\frac{n\pi}{a_p}\right)^2+ks_1\right)-(ks_1)^2}$$

It was suggested by Lee et al. [33] that the values of a_pt in Eqs. (25) and (26)range between 4 and 5. Because of absence of oscillating cosine and sine functions, Eqs. (25) and (26) converges more quickly because. The optimally value of a_pt is 4.7 [33].

4. Results and Discussion

The results of the simulations using MATLAB are presented in this section. Figure 9 presents the time history of the vertical displacement of the vehicle body using Bouc-Wen model. The figure shows that the highest displacement occurs at *t=0.4*. The figure depicts that within *0-4 sec*, there is a rapid increase from *0* to *0.14* m in the displacement of the vehicle body. Then it significantly decreases and follow by an increase before it reaches the stability at the initial displacement 0.1 m after *t=3*.

Figure 10 depicts the time history of the vertical displacement of the vehicle axle based on Bouc-Wen model. The axle attains it vertical displacement of the first oscillation at 0.17 m and its oscillation begins to damp out as time evolves until it reaches its stability from t=2.5 onwards.

Based on the modified Bouc-Wen model, Figure 11 illustrates the time history of the vertical displacement of the vehicle body. The body first attains its highest displacement and after their oscillations begins to damp out as time evolves until steady states and stability are reach.

It should be pointed that the results in Figures 9 and 10 show that the oscillation of the displacement of the axle is more fluctuating compared to the displacement of the body. This is due to the installation of the damper between the body and the axle in which the damper acts as shock-absorber.

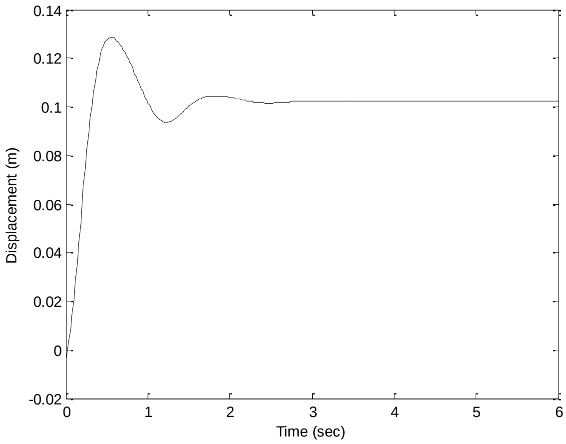

Figure 9. Time history of the Vertical Displacement of the Vehicle Body using Bouc-Wen Model

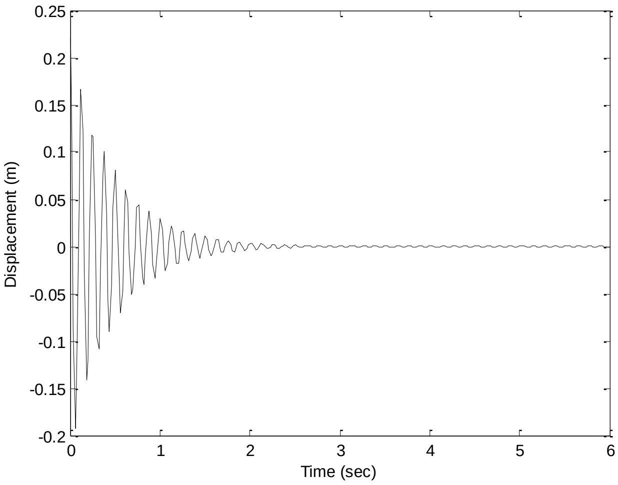

Figure 10. Time history of the Vertical Displacement of the Vehicle Axle using Bouc-Wen Model

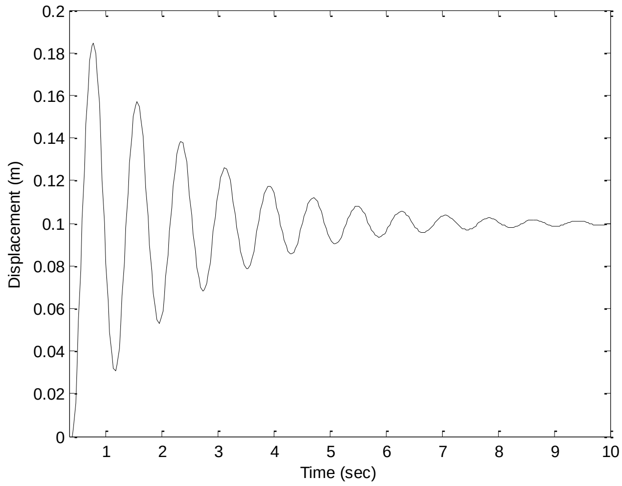

Figure 11. Time history of the Vertical Displacement of the Vehicle Body using Modified Bouc-Wen Model

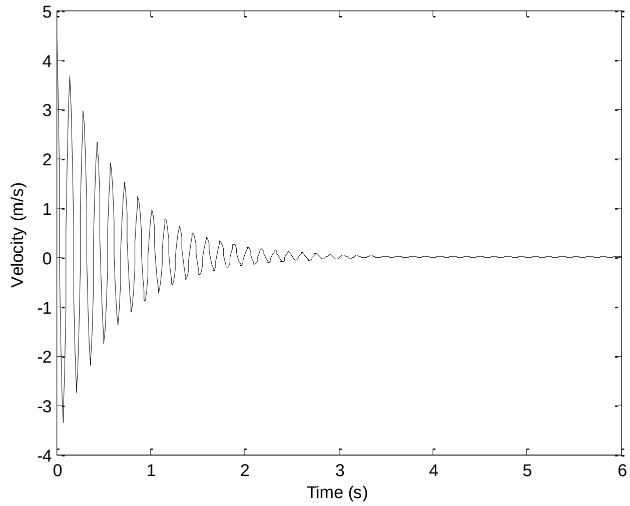

Figure 12. Time history of the Vertical Velocity of the Vehicle Axle using Bouc-Wen Model

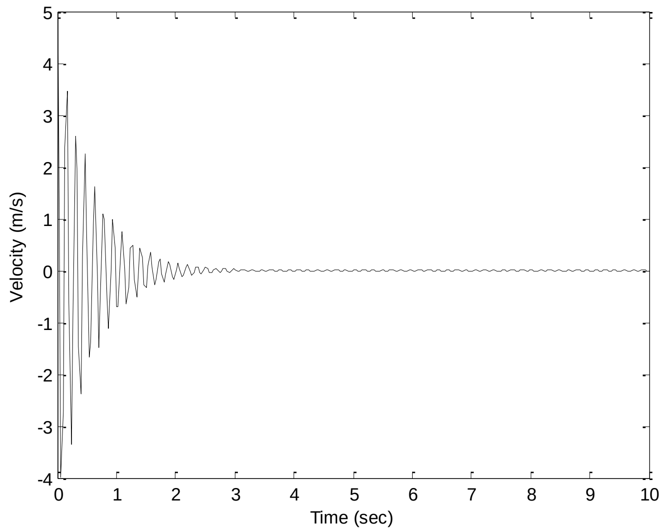

Figure 13. Time history of the Vertical Velocity of the Vehicle Axle using Modified Bouc-Wen Model

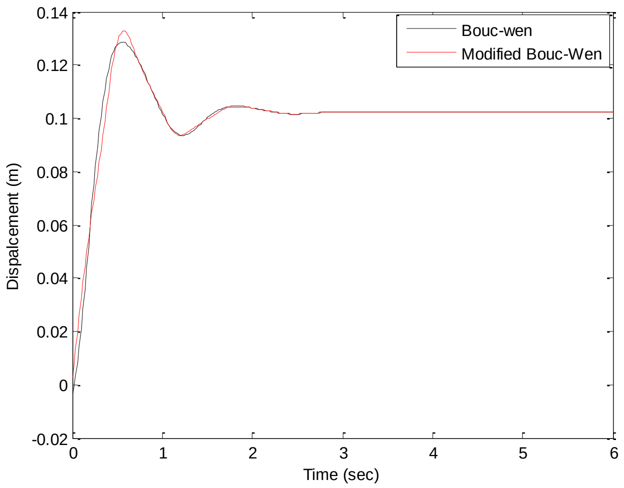

Figure 14. Comparison of Bouc-Wen Model and Modified Bouc-Wen Model for the Time history of the vertical displacement of the body

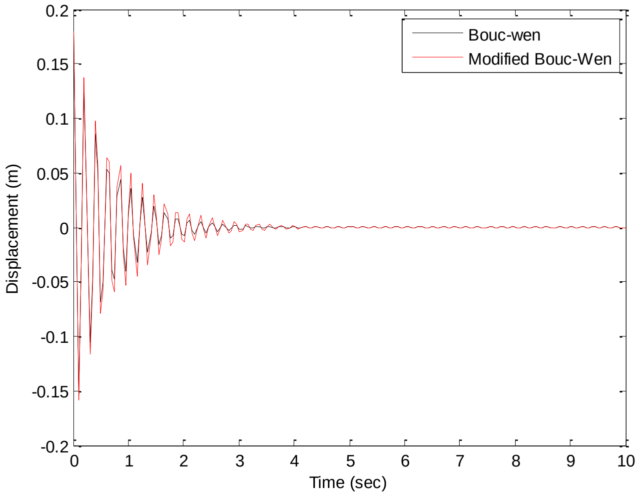

Figure 15. Comparison of Bouc-Wen Model and Modified Bouc-Wen Model for the Time history of the Vertical velocities of the axle

Figures 12 and 13 present the time histories of the vertical velocity of the vehicle body based on the Bouc-Wen and modified Bouc-Wen models, respective while Figures 14 and Figure 15 compare the time histories of Bouc-Wen Model and modified Bouc-Wen Model for the Time history of the vertical displacement and velocityof the axle. The figures show the variation between the two models. However, it was previously stated that the Bouc-Wen model cannot produce the experimentally observed roll-off in the yield region for velocities with a small absolute value and operational sign opposite to the sign of the acceleration. The results of the present study agree with the results of the numerical study of Viswanathan et al. [34].

5. Conclusion

The analytical solutions for the vehicle dynamic behaviour under the influence of magnetorheological fluid damper have been developed in this study. The models of a quarter vehicle were considered, and the damping force of the magnetorheological fluid damper were modelled using Bouc-Wen and modified Bouc-Wen models. Laplace transform method was used to develop analytical solutions for the dynamic equations. It was revealed that the presence of magnetorheological damper (which acts as a shock-absorber) between the body and the axle produced more fluctuating oscillation of the displacement of the axle compared to the displacement of the body. Moreover, the variation between the two models of Bouc-Wen and modified Bouc-Wen models is established. It is stated that the Bouc-Wen model cannot produce the experimentally observed roll-off in the yield region for velocities with a small absolute value and operational sign opposite to the sign of the acceleration. Therefore, the use of modified Bouc-Wen model is recommended. Also, the developed analytical solutions will serve as basis for comparison of any other method of analysis of the problem.

References

[1] Gysen, B. L., Paulides, J. J., Janssen, J. L., & Lomonova, E. A. (2010). Active electromagnetic suspension system for improved vehicle dynamics.IEEE Transactions on Vehicular Technology, 59(3), 1156-1163.

[2] Dave, W.)2015). The other active suspension cars. leyton house," pp. 1{6, June 2015. [Online]. Available: https://www.f1technical.net/forum/viewtopic.php?t=21478start=45
[3] Hrishikesh B. Z. (2017). Nonlinear design, modeling and simulation of magneto Rheological suspension: a control system and systems Engineering approach. Master Thesis, Purdue University.
[4] Jolly, M. R., Bender, J. W., and Carlson, J. D. (1998). Properties and Applications of Commercial Magnetorheological Fluids, in SPIE 5th Annual Int Symposium on Smart Structures and Materials, San Diego, CA.
[5] Wereley, N. M., Kamath, G. M., & Madhavan, V. (1999). Hysteresis modeling of semi-active magnetorheological helicopter dampers. Journal of intelligent material systems and structures, 10(8), 624-633.
[6] Ikhouane, F., & Dyke, S. J. (2007). Modeling and identification of a shear mode magnetorheological damper. Smart Materials and Structures, 16(3), 605.
[7] Jimnez, R., & Alvarez, L. (2002, December). Real time identification of structures with magnetorheological dampers. In Decision and Control, 2002, Proceedings of the 41st IEEE Conference on (Vol. 1, pp. 1017-1022).
[8] Sakai, C., Ohmori, H., & Sano, A. (2003, December). Modeling of MR damper with hysteresis for adaptive vibration control. In Decision and Control, 2003. Proceedings. 42nd IEEE Conference on (Vol. 4, pp. 3840-3845).
[9] Terasawa, T., Sakai, C., Ohmori, H., & Sano, A. (2004, December). Adaptive identification of MR damper for vibration control. In Decision and Control, 2004. CDC. 43rd IEEE Conference on (Vol. 3, pp. 2297-2303).
[10] Kwok, N. M., Ha, Q. P., Nguyen, T. H., Li, J., & Samali, B. (2006). A novel hysteretic model for magnetorheological fluid dampers and parameter identification using particle swarm optimization. Sensors and Actuators A: Physical, 132(2), 441-451.
[11] Wang, E. R., Ma, X. Q., Rakhela, S., & Su, C. Y. (2003). Modelling the hysteretic characteristics of a magnetorheological fluid damper. Proceedings of the Institution of Mechanical Engineers, Part D: Journal of Automobile Engineering, 217(7), 537-550.
[12] Ma, X. Q., Rakheja, S., & Su, C. Y. (2006). Relative assessments of current dependent models for magneto-rheological fluid dampers. In 2006 IEEE International Conference on Networking, Sensing and Control (pp. 510-515).
[13] Oh, H. U. (2004). Experimental demonstration of an improved magneto-rheological fluid damper for suppression of vibration of a space flexible structure. Smart materials and structures, 13(5), 12-38.
[14] Wang, L. X., & Kamath, H. (2006). Modelling hysteretic behaviour in magnetorheological fluids and dampers using phase-transition theory. Smart materials and structures, 15(6), 17-25.
[15] Spencer Jr., B. F., Dyke, S. J., Sain, and M. K. & Carlson, J. D. (1997). "Phenomenological model of a magnetorheological damper," ASCE Journal of Engineering Mechanics, Vol. 123(3), 230-238.
[16] Yang, G., Spencer, B. F., Carlson, J. D., & Sain, M. K. (2002). Large-scale MR fluid dampers: modeling and dynamic performance considerations. Engineering structures, 24(3), 309-323.
[17] Wereley, N. M., Pang, L., & Kamath, G. M. (1998). Idealized hysteresis modeling of electrorheological and magnetorheological dampers. Journal of Intelligent Material Systems and Structures, 9(8), 642-649.
[18] Pang, L., Kamath, G. M., & Wereley, N. M. (1998, April). Analysis and testing of a linear stroke magnetorheological damper. In Proc. 39th AIAA/ASME/ASCE/AHS/ASC Structures, Structural Dynamics, and Materials Conference and Exhibit and AIAA/ASME/AHS Adaptive Structures Forum (pp. 2841-2856).
[19] Snyder, R. A., Kamath, G. M., & Wereley, N. M. (2001). Characterization and analysis of magnetorheological damper behaviour under sinusoidal loading. AIAA journal, 39(7), 1240-1253.
[20] Spencer Jr., B. F., Dyke, S. J., Sain, and M. K. & Carlson, J. D. (1996). Carlson, Modelling and Control of Magnetorheological Dampers for Seismic Response Reduction. Smart materials and structures, 5(5), 565.
[21] Ma, X. Q., Rakheja, S., & Su, C. Y. (2007). Development and relative assessments of models for characterizing the current dependent hysteresis properties of magnetorheological fluid dampers. Journal of intelligent material systems and structures, 18(5), 487-502.
[22] Li, W. H., Yao, G. Z., Chen, G., Yeo, S. H., & Yap, F. F. (2000). Testing and steady state modeling of a linear MR damper under sinusoidal loading. Smart Materials and Structures, 9(1), 95.
[23] Choi, S. B., Lee, S. K., & Park, Y. P. (2001). A hysteresis model for the field-dependent damping force of a magnetorheological damper. Journal of Sound and Vibration, 245(2), 375-383.
[24] Song, X., Ahmadian, M., & Southward, S. C. (2005). Modeling magnetorheological dampers with application of nonparametric approach. Journal of Intelligent Material Systems and Structures, 16(5), 421-432.
[25] Huang, Y., Liu, X., & Chen, B. (2006, October). Autoregressive trispectral characteristics of magnetorheological damping device. In 2006 IEEE/RSJ International Conference on Intelligent Robots and Systems (pp. 5878-5882).
[26] Koga, K., & Sano, A. (2006, June). Query-based approach to prediction of MR damper force with application to vibration control. In 2006 American Control Conference (pp. 7-pp).
[27] Choi. S. B., Lee, B. K., Nam, M. H. and Cheong, C. C. (2000). Vibration control of a MR seat damper for commercial vehicles," Proceedings of SPIE Conference on Smart Structures and Materials: Smart Structures and Integrated Systems, SPIE 3985, 491-496.
[28] Li, W. H., Du, H., Chen, G., Yeo, S. H., & Guo, N. (2003). Nonlinear viscoelastic properties of MR fluids under large-amplitude-oscillatory-shear. *Rheologica Acta*, *42*(3), 280-286.

[29] Lai, C. Y. and Liao, W. H. "Vibration control of a suspension system via a magnetorheological fluid damper," Proceedings of the 5th European Conference on Smart Structures and Materials, SPIE, Vol. 4073, pp. 240-251, 2000.
[30] Patel, C. B., Gohil, P. P. and Borhade, B. (2010). Modelling and Vibration Analysis of a Road Profile Measuring System. International Journal of Automotive and Mechanical Engineering. 1, 13-28.
[31] Hiu Fung Lam, Wei-Hsin Liao, "Semi-active control of automotive suspension systems with magnetorheological dampers," Proc. SPIE 4327, Smart Structures and Materials 2001: Smart Structures and Integrated Systems, (16 August 2001); doi: 10.1117/12.436523
[32] Simon, R. M., Stroot, M. T., Weiss, G. H. (1972). Numerical inversion of Laplace transforms with application to percentage labeled mitoses experiments. Computers and Biomedical Research. 5, 596-607.
[33] Lee, S. T., Chien, M. C. H., Culham, W. E. Vertical single-well pulse testing of a three-layer stratified reservoir. SPE Annual Technical Conference and Exhibition. Society of Petroleum Engineers, Houston, Texas, 1984.
[34] Viswanathan, K. K., Tang, J. S., Aziz, Z.A. and Sambath, P. (2012) Mathematical Modeling of Magneto rheological Fluid Damper in the Semi-Active Suspension System. The 11th National Conference on Mathematical Techniques and Applications. AIP Conf. Proc.